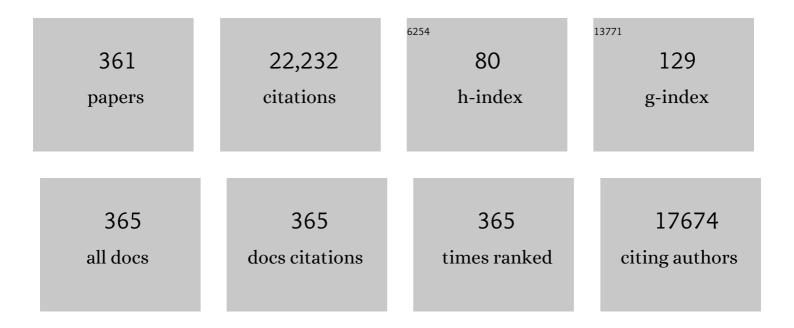
List of Publications by Year in descending order

Source: https://exaly.com/author-pdf/3047737/publications.pdf Version: 2024-02-01



FENC PAN

#	Article	IF	CITATIONS
1	Encoding the atomic structure for machine learning in materials science. Wiley Interdisciplinary Reviews: Computational Molecular Science, 2022, 12, e1558.	14.6	29
2	Coilâ€ŧo‣tretch Transition of Binder Chains Enabled by "Nanoâ€Combs―to Facilitate Highly Stable SiO _x Anode. Energy and Environmental Materials, 2022, 5, 1310-1316.	12.8	4
3	Superior cycling stability of H0.642V2O5·0.143H2O in rechargeable aqueous zinc batteries. Science China Materials, 2022, 65, 78-84.	6.3	12
4	Advanced Electron Energy Loss Spectroscopy for Battery Studies. Advanced Functional Materials, 2022, 32, 2107190.	14.9	26
5	Highâ€Performance Si Photocathode Enabled by Spatial Decoupling Multifunctional Layers for Water Splitting. Advanced Functional Materials, 2022, 32, 2107164.	14.9	15
6	Breaking the energy density limit of LiNiO2: Li2NiO3 or Li2NiO2?. Science China Materials, 2022, 65, 913-919.	6.3	6
7	Co ₄ Nâ€Decorated 3D Woodâ€Derived Carbon Host Enables Enhanced Cathodic Electrocatalysis and Homogeneous Lithium Deposition for Lithium–Sulfur Full Cells. Small, 2022, 18, e2105664.	10.0	34
8	Heavy Fluorination via Ion Exchange Achieves Highâ€Performance Li–Mn–O–F Layered Cathode for Liâ€Ion Batteries. Small, 2022, 18, e2103499.	10.0	10
9	Influence of electrolyte structural evolution on battery applications: Cationic aggregation from dilute to high concentration. Aggregate, 2022, 3, .	9.9	37
10	Li-rich channels as the material gene for facile lithium diffusion in halide solid electrolytes. EScience, 2022, 2, 79-86.	41.6	28
11	Defect-mediated Jahn-Teller effect in layered LiNiO2. Science China Materials, 2022, 65, 1696-1700.	6.3	8
12	Thiotetrelates Li ₂ ZnXS ₄ (X = Si, Ge, and Sn) As Potential Li-Ion Solid-State Electrolytes. ACS Applied Materials & Interfaces, 2022, 14, 9203-9211.	8.0	2
13	Tailoring the coercive field in ferroelectric metal-free perovskites by hydrogen bonding. Nature Communications, 2022, 13, 794.	12.8	24
14	Graph-based discovery and analysis of atomic-scale one-dimensional materials. National Science Review, 2022, 9, .	9.5	5
15	Automating Materials Exploration with a Semantic Knowledge Graph for Liâ€lon Battery Cathodes. Advanced Functional Materials, 2022, 32, .	14.9	16
16	Bioâ€Inspired Binder Design for a Robust Conductive Network in Siliconâ€Based Anodes. Small Methods, 2022, 6, e2101591.	8.6	23
17	Enhanced Ferroelectric and Piezoelectric Properties in Graphene-Electroded Pb(Zr,Ti)O ₃ Thin Films. ACS Applied Materials & Interfaces, 2022, 14, 17987-17994.	8.0	5
18	Tuning core-shell structural architecture for high-performance Li-Mn-O layered oxides. Nano Energy, 2022, 96, 107092.	16.0	5

#	Article	IF	CITATIONS
19	Scalable Lithiophilic/Sodiophilic Porous Buffer Layer Fabrication Enables Uniform Nucleation and Growth for Lithium/Sodium Metal Batteries. Advanced Functional Materials, 2022, 32, .	14.9	21
20	Surface Design with Cation and Anion Dual Gradient Stabilizes Highâ€Voltage LiCoO ₂ . Advanced Energy Materials, 2022, 12, .	19.5	36
21	Delocalized Li@Mn6 superstructure units enable layer stability of high-performance Mn-rich cathode materials. CheM, 2022, 8, 2163-2178.	11.7	19
22	Progress in interface structure and modification of zinc anode for aqueous batteries. Nano Energy, 2022, 98, 107333.	16.0	93
23	Origin and regulation of oxygen redox instability in high-voltage battery cathodes. Nature Energy, 2022, 7, 808-817.	39.5	55
24	Intercalation-driven ferroelectric-to-ferroelastic conversion in a layered hybrid perovskite crystal. Nature Communications, 2022, 13, .	12.8	27
25	Elastic Lattice Enabling Reversible Tetrahedral Li Storage Sites in a Highâ€Capacity Manganese Oxide Cathode. Advanced Materials, 2022, 34, .	21.0	15
26	Strategies and characterization methods for achieving high performance PEO-based solid-state lithium-ion batteries. Chemical Communications, 2022, 58, 8182-8193.	4.1	24
27	Biomimetic Lipidâ€Bilayer Anode Protection for Long Lifetime Aqueous Zincâ€Metal Batteries. Advanced Functional Materials, 2022, 32, .	14.9	16
28	Origin of structural degradation in Li-rich layered oxide cathode. Nature, 2022, 606, 305-312.	27.8	206
29	Promoting the performances of P2-type sodium layered cathode by inducing Na site rearrangement. Nano Energy, 2022, 100, 107482.	16.0	25
30	The Interfacial Properties of Monolayer MX–Metal Contacts. Journal of Electronic Materials, 2022, 51, 4824-4835.	2.2	3
31	Band-Structure Engineering of Copper Benzenehexathiol for Reversible Mechanochromism: A First-Principles Study. Journal of Physical Chemistry C, 2022, 126, 11642-11651.	3.1	0
32	3D Hierarchical Grapheneâ€CNT Anode for Sodiumâ€Ion Batteries: a Firstâ€Principles Assessment. Advanced Theory and Simulations, 2022, 5, .	2.8	1
33	Boosting the Energy Density of Aqueous Batteries via Facile Grotthuss Proton Transport. Angewandte Chemie, 2021, 133, 4215-4220.	2.0	27
34	Structure and Properties of Prussian Blue Analogues in Energy Storage and Conversion Applications. Advanced Functional Materials, 2021, 31, 2006970.	14.9	238
35	Valence state of transition metal center as an activity descriptor for CO2 reduction on single atom catalysts. Journal of Energy Chemistry, 2021, 56, 444-448.	12.9	20
36	Tuning Zn2+ coordination environment to suppress dendrite formation for high-performance Zn-ion batteries. Nano Energy, 2021, 80, 105478.	16.0	318

#	Article	IF	CITATIONS
37	Optimizing Ion Pathway in Titanium Carbide MXene for Practical Highâ€Rate Supercapacitor. Advanced Energy Materials, 2021, 11, 2003025.	19.5	152
38	Atomic/nano-scale in-situ probing the shuttling effect of redox mediator in Na–O2 batteries. Journal of Energy Chemistry, 2021, 56, 438-443.	12.9	7
39	Boosting the Energy Density of Aqueous Batteries via Facile Grotthuss Proton Transport. Angewandte Chemie - International Edition, 2021, 60, 4169-4174.	13.8	116
40	Deciphering the Oxygen Absorption Preâ€edge: A Caveat on its Application for Probing Oxygen Redox Reactions in Batteries. Energy and Environmental Materials, 2021, 4, 246-254.	12.8	56
41	Co13O8—metalloxocubes: a new class of perovskite-like neutral clusters with cubic aromaticity. National Science Review, 2021, 8, nwaa201.	9.5	21
42	Discovering a New class of fluoride solid-electrolyte materials via screening the structural property of Li-ion sublattice. Nano Energy, 2021, 79, 105407.	16.0	24
43	Improvement of alkali metal ion batteries <i>via</i> interlayer engineering of anodes: from graphite to graphene. Nanoscale, 2021, 13, 12521-12533.	5.6	14
44	Structure evolution and energy storage mechanism of Zn ₃ V ₃ O ₈ spinel in aqueous zinc batteries. Nanoscale, 2021, 13, 14408-14416.	5.6	17
45	Tuning the exposure of BiVO ₄ -{010} facets to enhance the N ₂ photofixation performance. RSC Advances, 2021, 11, 28908-28911.	3.6	3
46	Optimizing the sulfonic groups of a polymer to coat the zinc anode for dendrite suppression. Chemical Communications, 2021, 57, 5326-5329.	4.1	30
47	Interplay between multiple doping elements in high-voltage LiCoO ₂ . Journal of Materials Chemistry A, 2021, 9, 5702-5710.	10.3	33
48	Vanadium Cluster Neutrals Reacting with Water: Superatomic Features and Hydrogen Evolution in a Fishing Mode. Journal of Physical Chemistry Letters, 2021, 12, 1593-1600.	4.6	21
49	Simultaneously Regulating Uniform Zn2+ Flux and Electron Conduction by MOF/rGO Interlayers for High-Performance Zn Anodes. Nano-Micro Letters, 2021, 13, 73.	27.0	106
50	Topological representations of crystalline compounds for the machine-learning prediction of materials properties. Npj Computational Materials, 2021, 7, .	8.7	36
51	Structural origin of the high-voltage instability of lithium cobalt oxide. Nature Nanotechnology, 2021, 16, 599-605.	31.5	148
52	Understanding Co roles towards developing Co-free Ni-rich cathodes for rechargeable batteries. Nature Energy, 2021, 6, 277-286.	39.5	255
53	A Programmable and Automated Platform for Integrated Synthesis and Evaluation of Water Electrolysis Catalysts. Advanced Materials Technologies, 2021, 6, 2001036.	5.8	3
54	Construction and Application of Materials Knowledge Graph Based on Author Disambiguation: Revisiting the Evolution of LiFePO ₄ . Advanced Energy Materials, 2021, 11, 2003580.	19.5	16

#	Article	IF	CITATIONS
55	Cycling mechanism of Li2MnO3: Li–CO2Âbatteries and commonality on oxygen redox in cathode materials. Joule, 2021, 5, 975-997.	24.0	88
56	Interactions are important: Linking multi-physics mechanisms to the performance and degradation of solid-state batteries. Materials Today, 2021, 49, 145-183.	14.2	51
57	Schottky barrier heights in two-dimensional field-effect transistors: from theory to experiment. Reports on Progress in Physics, 2021, 84, 056501.	20.1	97
58	Constructing a Highly Efficient Aligned Conductive Network to Facilitate Depolarized Highâ€Arealâ€Capacity Electrodes in Liâ€Ion Batteries. Advanced Energy Materials, 2021, 11, 2100601.	19.5	38
59	Progressive "Layer to Hybrid Spinel/Layer―Phase Evolution with Proton and Zn ²⁺ Co-intercalation to Enable High Performance of MnO ₂ -Based Aqueous Batteries. ACS Applied Materials & Interfaces, 2021, 13, 22466-22474.	8.0	13
60	Twin boundary defect engineering improves lithium-ion diffusion for fast-charging spinel cathode materials. Nature Communications, 2021, 12, 3085.	12.8	77
61	The role of M@Ni6 superstructure units in honeycomb-ordered layered oxides for Li/Na ion batteries. Nano Energy, 2021, 83, 105834.	16.0	15
62	Is graphite nanomesh a promising anode for the Na/K-Ions batteries?. Carbon, 2021, 176, 242-252.	10.3	28
63	Algebraic graph-assisted bidirectional transformers for molecular property prediction. Nature Communications, 2021, 12, 3521.	12.8	76
64	Oxygen-Deficient β-MnO2@Graphene Oxide Cathode for High-Rate and Long-Life Aqueous Zinc Ion Batteries. Nano-Micro Letters, 2021, 13, 173.	27.0	89
65	Atomically dispersed S-Fe-N4 for fast kinetics sodium-sulfur batteries via a dual function mechanism. Cell Reports Physical Science, 2021, 2, 100531.	5.6	31
66	Modifying Li@Mn ₆ Superstructure Units by Al Substitution to Enhance the Longâ€Cycle Performance of Coâ€Free Liâ€Rich Cathode. Advanced Energy Materials, 2021, 11, 2101962.	19.5	39
67	PIMâ€l as a Multifunctional Framework to Enable Highâ€Performance Solidâ€State Lithium–Sulfur Batteries. Advanced Functional Materials, 2021, 31, 2104830.	14.9	47
68	Sub-10Ânm two-dimensional transistors: Theory and experiment. Physics Reports, 2021, 938, 1-72.	25.6	80
69	Constructing a Resilient Hierarchical Conductive Network to Promote Cycling Stability of SiO <i>_x</i> Anode via Binder Design. Small, 2021, 17, e2102256.	10.0	17
70	Synergistic Dissociationâ€andâ€Trapping Effect to Promote Liâ€lon Conduction in Polymer Electrolytes via Oxygen Vacancies. Small, 2021, 17, e2102039.	10.0	38
71	Distinct Oxygen Redox Activities in Li ₂ MO ₃ (M = Mn, Ru, Ir). ACS Energy Letters, 2021, 6, 3417-3424.	17.4	33
72	Recent Advances and Perspective on Electrochemical Ammonia Synthesis under Ambient Conditions. Small Methods, 2021, 5, e2100460.	8.6	33

1

#	ARTICLE	IF	CITATIONS
73	Controlled Experiments and Optimized Theory of Absorption Spectra of Li Metal and Salts. ACS Applied Materials & Interfaces, 2021, 13, 45488-45495.	8.0	8
74	Suppressing Polysulfide Shuttling in Lithium–Sulfur Batteries via a Multifunctional Conductive Binder. Small Methods, 2021, 5, e2100839.	8.6	14
75	Inherent inhibition of oxygen loss by regulating superstructural motifs in anionic redox cathodes. Nano Energy, 2021, 88, 106252.	16.0	32
76	Recent progress in Li and Mn rich layered oxide cathodes for Li-ion batteries. Journal of Energy Chemistry, 2021, 61, 368-385.	12.9	43
77	Tunning the linkage of structure units to enable stable spinel-based cathode in the wide potential window. Nano Energy, 2021, 89, 106457.	16.0	5
78	Understanding Li-ion thermodynamic and kinetic behaviors in concentrated electrolyte for the development of aqueous lithium-ion batteries. Nano Energy, 2021, 89, 106413.	16.0	13
79	P2/O3 biphasic Fe/Mn-based layered oxide cathode with ultrahigh capacity and great cyclability for sodium ion batteries. Nano Energy, 2021, 90, 106504.	16.0	69
80	Precision grain boundary engineering in commercial Bi ₂ Te _{2.7} Se _{0.3} thermoelectric materials towards high performance. Journal of Materials Chemistry A, 2021, 9, 11442-11449.	10.3	26
81	From bulk to interface: electrochemical phenomena and mechanism studies in batteries <i>via</i> electrochemical quartz crystal microbalance. Chemical Society Reviews, 2021, 50, 10743-10763.	38.1	48
82	In-Situ Polymerized Binder: A Three-in-One Design Strategy for All-Integrated SiO <i>_{<i>x</i>}</i> Anode with High Mass Loading in Lithium Ion Batteries. ACS Energy Letters, 2021, 6, 290-297.	17.4	92
83	Impact of Electrolyte Salts on Na Storage Performance for High-Surface-Area Carbon Anodes. ACS Applied Materials & Interfaces, 2021, 13, 48745-48752.	8.0	8
84	Tuning Site Energy by XO ₆ Units in LiX ₂ (PO ₄) ₃ Enables High Li Ion Conductivity and Improved Stability. ACS Applied Materials & Interfaces, 2021, 13, 50948-50956.	8.0	7
85	Revealing Roles of Co and Ni in Mnâ€Rich Layered Cathodes. Advanced Energy Materials, 2021, 11, .	19.5	24
86	Highly Distorted Grain Boundary with an Enhanced Carrier/Phonon Segregation Effect Facilitates High-Performance Thermoelectric Materials. ACS Applied Materials & Interfaces, 2021, 13, 51018-51027.	8.0	13
87	Extracting Predictive Representations from Hundreds of Millions of Molecules. Journal of Physical Chemistry Letters, 2021, 12, 10793-10801.	4.6	28
88	Potential Solid-State Electrolytes with Good Balance between Ionic Conductivity and Electrochemical Stability: Li _{5–<i>x</i>} M _{1–<i>x</i>} M _X AAA <td>= Asl)otj etc</td> <td>ეඅ©000 rgB⊺</td>	= Asl)otj etc	ეඅ©000 rgB⊺
89	In situ Raman spectroscopyÂreveals the structure and dissociation of interfacial water. Nature, 2021, 600, 81-85.	27.8	381

90Reducing parasitic absorption and recombination losses in silicon solar cells through transition
metal doped glass frit. Functional Materials Letters, 2020, 13, 1950087.1.2

#	Article	IF	CITATIONS
91	Efficient Ni ₂ Co ₄ P ₃ Nanowires Catalysts Enhance Ultrahigh‣oading Lithium–Sulfur Conversion in a Microreactor‣ike Battery. Advanced Functional Materials, 2020, 30, 1906661.	14.9	134
92	Revealing the anion intercalation behavior and surface evolution of graphite in dual-ion batteries via in situ AFM. Nano Research, 2020, 13, 412-418.	10.4	33
93	High-throughput HSE study on the doping effect in anatase TiO ₂ . Physical Chemistry Chemical Physics, 2020, 22, 39-53.	2.8	30
94	Revealing cooperative Li-ion migration in Li _{1+x} Al _x Ti _{2â^'x} (PO ₄) ₃ solid state electrolytes with high Al doping. Journal of Materials Chemistry A, 2020, 8, 342-348.	10.3	41
95	The stability and reaction mechanism of a LiF/electrolyte interface: insight from density functional theory. Journal of Materials Chemistry A, 2020, 8, 2613-2617.	10.3	13
96	Enhanced thermoelectric performance through optimizing structure of anionic framework in AgCuTe-based materials. Chemical Engineering Journal, 2020, 386, 123917.	12.7	16
97	â€~Structure units' as material genes in cathode materials for lithium-ion batteries. National Science Review, 2020, 7, 242-245.	9.5	31
98	Atomic-scale tuning of oxygen-doped Bi ₂ Te _{2.7} Se _{0.3} to simultaneously enhance the Seebeck coefficient and electrical conductivity. Nanoscale, 2020, 12, 1580-1588.	5.6	23
99	Quasi-solid single Zn-ion conductor with high conductivity enabling dendrite-free Zn metal anode. Energy Storage Materials, 2020, 27, 1-8.	18.0	91
100	Tuning Rate-Limiting Factors to Achieve Ultrahigh-Rate Solid-State Sodium-Ion Batteries. ACS Applied Materials & Interfaces, 2020, 12, 48677-48683.	8.0	15
101	Charge transport mechanisms in potassium superoxide. Physical Chemistry Chemical Physics, 2020, 22, 24480-24489.	2.8	6
102	Laser writing of the restacked titanium carbide MXene for high performance supercapacitors. Energy Storage Materials, 2020, 32, 418-424.	18.0	31
103	Achieving High Thermoelectric Performance by Introducing 3D Atomically Thin Conductive Framework in Porous Bi ₂ Te _{2.7} Se _{0.3} â€Carbon Nanotube Hybrids. Advanced Electronic Materials, 2020, 6, 2000292.	5.1	8
104	Enhanced long-term cyclability in Li-Rich layered oxides by electrochemically constructing a LixTM3-xO4-type spinel shell. Nano Energy, 2020, 77, 105188.	16.0	29
105	Double the Capacity of Manganese Spinel for Lithiumâ€ion Storage by Suppression of Cooperative Jahn–Teller Distortion. Advanced Energy Materials, 2020, 10, 2000363.	19.5	75
106	Optimizing the structure of layered cathode material for higher electrochemical performance by elucidating structural evolution during heat processing. Nano Energy, 2020, 78, 105194.	16.0	19
107	Ultrafast solid-liquid intercalation enabled by targeted microwave energy delivery. Science Advances, 2020, 6, .	10.3	12
108	Preintercalation Strategy in Manganese Oxides for Electrochemical Energy Storage: Review and Prospects. Advanced Materials, 2020, 32, e2002450.	21.0	127

#	Article	IF	CITATIONS
109	Tuning Single-Atom Catalysts of Nitrogen-Coordinated Transition Metals for Optimizing Oxygen Evolution and Reduction Reactions. Journal of Physical Chemistry C, 2020, 124, 13168-13176.	3.1	43
110	Intrinsic role of ↑↑↑'↑'-type magnetic structure on magnetoelectric coupling in Y2NiMnO6. Applied Physics Letters, 2020, 116, 242901.	3.3	3
111	Harnessing the surface structure to enable high-performance cathode materials for lithium-ion batteries. Chemical Society Reviews, 2020, 49, 4667-4680.	38.1	88
112	Structure and performance of the LiFePO ₄ cathode material: from the bulk to the surface. Nanoscale, 2020, 12, 15036-15044.	5.6	59
113	An Interfaceâ€Bridged Organic–Inorganic Layer that Suppresses Dendrite Formation and Side Reactions for Ultra‣ong‣ife Aqueous Zinc Metal Anodes. Angewandte Chemie, 2020, 132, 16737-16744.	2.0	52
114	An Interfaceâ€Bridged Organic–Inorganic Layer that Suppresses Dendrite Formation and Side Reactions for Ultraâ€Longâ€Life Aqueous Zinc Metal Anodes. Angewandte Chemie - International Edition, 2020, 59, 16594-16601.	13.8	270
115	Full Energy Range Resonant Inelastic X-ray Scattering of O ₂ and CO ₂ : Direct Comparison with Oxygen Redox State in Batteries. Journal of Physical Chemistry Letters, 2020, 11, 2618-2623.	4.6	30
116	Strong influence of strain gradient on lithium diffusion: flexo-diffusion effect. Nanoscale, 2020, 12, 15175-15184.	5.6	9
117	Sub-5 nm monolayer germanium selenide (GeSe) MOSFETs: towards a high performance and stable device. Nanoscale, 2020, 12, 15443-15452.	5.6	27
118	Polymer matrix mediated solvation of LiNO3 in carbonate electrolytes for quasi-solid high-voltage lithium metal batteries. Nano Research, 2020, 13, 2431-2437.	10.4	31
119	Hybridizing Li@Mn6 and Sb@Ni6 superstructure units to tune the electrochemical performance of Li-rich layered oxides. Nano Energy, 2020, 77, 105157.	16.0	10
120	Ultrahigh Capacity of Monolayer Dumbbell C ₄ N as a Promising Anode Material for Lithium-Ion Battery. Journal of the Electrochemical Society, 2020, 167, 020538.	2.9	11
121	Dissociate lattice oxygen redox reactions from capacity and voltage drops of battery electrodes. Science Advances, 2020, 6, eaaw3871.	10.3	82
122	Liâ€Ion Cooperative Migration and Oxyâ€&ulfide Synergistic Effect in Li ₁₄ P ₂ Ge ₂ S _{16â^6} <i>_x</i> O <i>_x<!--</td--><td>0.0ki</td><td>27</td></i>	0.0ki	27
123	Defect Engineering in Titanium-Based Oxides for Electrochemical Energy Storage Devices. Electrochemical Energy Reviews, 2020, 3, 286-343.	25.5	52
124	Achieving Both High Ionic Conductivity and High Interfacial Stability with the Li2+xC1–xBxO3 Solid-State Electrolyte: Design from Theoretical Calculations. ACS Applied Materials & Interfaces, 2020, 12, 6007-6014.	8.0	17
125	Recent advances in zinc anodes for high-performance aqueous Zn-ion batteries. Nano Energy, 2020, 70, 104523.	16.0	466
126	Stable Interface between Lithium and Electrolyte Facilitated by a Nanocomposite Protective Layer. Small Methods, 2020, 4, 1900751.	8.6	33

#	Article	IF	CITATIONS
127	Corrosion-resistant plasma electrolytic oxidation coating modified by Zinc phosphate and self-healing mechanism in the salt-spray environment. Surface and Coatings Technology, 2020, 384, 125321.	4.8	24
128	Neural Network Force Fields for Metal Growth Based on Energy Decompositions. Journal of Physical Chemistry Letters, 2020, 11, 1364-1369.	4.6	7
129	The role of anions on the Helmholtz Plane for the solid-liquid interface in aqueous rechargeable lithium batteries. Nano Energy, 2020, 74, 104864.	16.0	27
130	Topology-Based Machine Learning Strategy for Cluster Structure Prediction. Journal of Physical Chemistry Letters, 2020, 11, 4392-4401.	4.6	25
131	Negligible voltage hysteresis with strong anionic redox in conventional battery electrode. Nano Energy, 2020, 74, 104831.	16.0	72
132	An Anionicâ€MOFâ€Based Bifunctional Separator for Regulating Lithium Deposition and Suppressing Polysulfides Shuttle in Li–S Batteries. Small Methods, 2020, 4, 2000082.	8.6	110
133	Tunable p- and n-type Nb:TiO ₂ and performance optimizing of self-powered Nb:TiO ₂ /CdS photodetectors. Semiconductor Science and Technology, 2020, 35, 075015.	2.0	3
134	Wannier–Koopmans method calculations for transition metal oxide band gaps. Npj Computational Materials, 2020, 6, .	8.7	11
135	Holey graphite: A promising anode material with ultrahigh storage for lithium-ion battery. Electrochimica Acta, 2020, 346, 136244.	5.2	49
136	Monolayer Honeycomb Borophene: A Promising Anode Material with a Record Capacity for Lithium-Ion and Sodium-Ion Batteries. Journal of the Electrochemical Society, 2020, 167, 090527.	2.9	28
137	Highly Dispersed Cobalt Clusters in Nitrogenâ€Đoped Porous Carbon Enable Multiple Effects for Highâ€Performance Li–S Battery. Advanced Energy Materials, 2020, 10, 1903550.	19.5	192
138	Wavelength-Dependent Solar N ₂ Fixation into Ammonia and Nitrate in Pure Water. Research, 2020, 2020, 3750314.	5.7	30
139	Structural and optoelectrical properties of Nb-TiO2 films fabricated by low-energy magnetron sputtering and post-annealing. Surface and Coatings Technology, 2019, 365, 10-14.	4.8	6
140	Improved electrochemical performance of LiNi0.5Mn0.3Co0.2O ₂ electrodes coated by atomic-layer-deposited Ta ₂ O ₅ . Functional Materials Letters, 2019, 12, 1850103.	1.2	7
141	Revealing magnetic ground state of a layered cathode material by muon spin relaxation and neutron scattering experiments. Applied Physics Letters, 2019, 114, 203901.	3.3	4
142	Anisotropic interfacial properties of monolayer GeSe—metal contacts. Semiconductor Science and Technology, 2019, 34, 095021.	2.0	7
143	Revealing Insights into Li _{<i>x</i>} FePO ₄ Nanocrystals with Magnetic Order at Room Temperature Resulting in Trapping of Li Ions. Journal of Physical Chemistry Letters, 2019, 10, 4794-4799.	4.6	7
144	Artificial Solid-Electrolyte Interface Facilitating Dendrite-Free Zinc Metal Anodes via Nanowetting Effect. ACS Applied Materials & Interfaces, 2019, 11, 32046-32051.	8.0	223

#	Article	IF	CITATIONS
145	Overwhelming the Performance of Single Atoms with Atomic Clusters for Platinum-Catalyzed Hydrogen Evolution. ACS Catalysis, 2019, 9, 8213-8223.	11.2	68
146	Tuning phase evolution of β-MnO2 during microwave hydrothermal synthesis for high-performance aqueous Zn ion battery. Nano Energy, 2019, 64, 103942.	16.0	154
147	Corrosion behavior of ZnO-reinforced coating on aluminum alloy prepared by plasma electrolytic oxidation. Surface and Coatings Technology, 2019, 374, 1015-1023.	4.8	20
148	Correlation between manganese dissolution and dynamic phase stability in spinel-based lithium-ion battery. Nature Communications, 2019, 10, 4721.	12.8	182
149	Alkali-Metal Anodes: From Lab to Market. Joule, 2019, 3, 2334-2363.	24.0	247
150	Cooling Induced Surface Reconstruction during Synthesis of Highâ€Ni Layered Oxides. Advanced Energy Materials, 2019, 9, 1901915.	19.5	34
151	Unravelling H ⁺ /Zn ²⁺ Synergistic Intercalation in a Novel Phase of Manganese Oxide for Highâ€Performance Aqueous Rechargeable Battery. Small, 2019, 15, e1904545.	10.0	133
152	A new single-particle model to evaluate the Li-ions diffusion coefficients of LiMn1â~'xFe _{<i>x</i>} PO ₄ . Functional Materials Letters, 2019, 12, 1950071.	1.2	1
153	An Ordered Ni ₆ â€Ring Superstructure Enables a Highly Stable Sodium Oxide Cathode. Advanced Materials, 2019, 31, e1903483.	21.0	65
154	Synthetic control of Prussian blue derived nano-materials for energy storage and conversion application. Materials Today Energy, 2019, 14, 100332.	4.7	28
155	Electrochemical Nitrogen Reduction Reaction Performance of Single-Boron Catalysts Tuned by MXene Substrates. Journal of Physical Chemistry Letters, 2019, 10, 6984-6989.	4.6	120
156	Tiâ€Gradient Doping to Stabilize Layered Surface Structure for High Performance Highâ€Ni Oxide Cathode of Liâ€Ion Battery. Advanced Energy Materials, 2019, 9, 1901756.	19.5	169
157	Tuning the Electrochemical Performance of Titanium Carbide MXene by Controllable In Situ Anodic Oxidation. Angewandte Chemie - International Edition, 2019, 58, 17849-17855.	13.8	117
158	Insight into Al–Si interface of PERC by Kelvin probe force microscopy. Functional Materials Letters, 2019, 12, 1950078.	1.2	1
159	Rare-earth element doping in glass frit for improved performance in silicon solar cells. Functional Materials Letters, 2019, 12, 1950080.	1.2	3
160	DMAP-Induced Gallium Phosphites with Different Dimensionality. Crystal Growth and Design, 2019, 19, 6011-6016.	3.0	4
161	Oxygen vacancy-rich MoO _{3â~x} nanobelts for photocatalytic N ₂ reduction to NH ₃ in pure water. Catalysis Science and Technology, 2019, 9, 803-810.	4.1	71
162	High throughput identification of Li ion diffusion pathways in typical solid state electrolytes and electrode materials by BV-Ewald method. Journal of Materials Chemistry A, 2019, 7, 1300-1306.	10.3	12

#	Article	IF	CITATIONS
163	Insights into Li/Ni ordering and surface reconstruction during synthesis of Ni-rich layered oxides. Journal of Materials Chemistry A, 2019, 7, 513-519.	10.3	92
164	Electron polarons in the subsurface layer of Mo/W-doped BiVO ₄ surfaces. RSC Advances, 2019, 9, 819-823.	3.6	8
165	Tuning polaronic redox behavior in olivine phosphate. Physical Chemistry Chemical Physics, 2019, 21, 4578-4583.	2.8	12
166	Designing Flexible Lithium-Ion Batteries by Structural Engineering. ACS Energy Letters, 2019, 4, 690-701.	17.4	175
167	Role of Superexchange Interactions on the Arrangement of Fe and Mn in LiMn _{<i>x</i>} Fe _{1–<i>x</i>} PO ₄ . Journal of Physical Chemistry C, 2019, 123, 17002-17009.	3.1	6
168	Low-Temperature Catalytic Graphitization to Enhance Na-Ion Transportation in Carbon Electrodes. ACS Applied Materials & Interfaces, 2019, 11, 24164-24171.	8.0	27
169	Ni/Li Disordering in Layered Transition Metal Oxide: Electrochemical Impact, Origin, and Control. Accounts of Chemical Research, 2019, 52, 2201-2209.	15.6	315
170	Interfacial Properties of Monolayer Antimonene Devices. Physical Review Applied, 2019, 11, .	3.8	22
171	Excellent Device Performance of Subâ€5â€nm Monolayer Tellurene Transistors. Advanced Electronic Materials, 2019, 5, 1900226.	5.1	65
172	LiAl5O8 as a potential coating material in lithium-ion batteries: a first principles study. Physical Chemistry Chemical Physics, 2019, 21, 13758-13765.	2.8	17
173	Cooperative transport enabling fast Li-ion diffusion in Thio-LISICON Li10SiP2S12 solid electrolyte. Nano Energy, 2019, 62, 844-852.	16.0	42
174	Tuning Li-enrichment in high-Ni layered oxide cathodes to optimize electrochemical performance for Li-ion battery. Nano Energy, 2019, 62, 709-717.	16.0	33
175	Identify crystal structures by a new paradigm based on graph theory for building materials big data. Science China Chemistry, 2019, 62, 982-986.	8.2	12
176	A new MaterialGo database and its comparison with other high-throughput electronic structure databases for their predicted energy band gaps. Science China Technological Sciences, 2019, 62, 1423-1430.	4.0	29
177	Monolayer GaS with high ion mobility and capacity as a promising anode battery material. Journal of Materials Chemistry A, 2019, 7, 14042-14050.	10.3	32
178	A bi-functional redox mediator promoting the ORR and OER in non-aqueous Li–O ₂ batteries. Chemical Communications, 2019, 55, 6567-6570.	4.1	12
179	Building ultraconformal protective layers on both secondary and primary particles of layered lithium transition metal oxide cathodes. Nature Energy, 2019, 4, 484-494.	39.5	345
180	Lithium ion diffusion mechanism in covalent organic framework based solid state electrolyte. Physical Chemistry Chemical Physics, 2019, 21, 9883-9888.	2.8	28

#	Article	IF	CITATIONS
181	A Versatile Polymeric Precursor to Highâ€Performance Silicon Composite Anode for Lithiumâ€Ion Batteries. Energy Technology, 2019, 7, 1900239.	3.8	8
182	Seed-Mediated Growth of Conductive and Transparent Anatase Nb-TiO ₂ Films for CdS-Based Devices. ACS Applied Nano Materials, 2019, 2, 1802-1807.	5.0	0
183	Scalable preparation of hierarchical porous activated carbon/graphene composites for high-performance supercapacitors. Journal of Materials Chemistry A, 2019, 7, 10058-10066.	10.3	19
184	Intrinsic Role of Cationic Substitution in Tuning Li/Ni Mixing in High-Ni Layered Oxides. Chemistry of Materials, 2019, 31, 2731-2740.	6.7	85
185	Hierarchically porous activated carbons derived from Schefflera octophylla leaves for high performance supercapacitors. Materials Letters, 2019, 247, 102-105.	2.6	11
186	Unusual Fermi‣evel Pinning and Ohmic Contact at Monolayer Bi 2 O 2 Se–Metal Interface. Advanced Theory and Simulations, 2019, 2, 1800178.	2.8	20
187	Revealing the Short ircuiting Mechanism of Garnetâ€Based Solidâ€State Electrolyte. Advanced Energy Materials, 2019, 9, 1900671.	19.5	163
188	A descriptor of "material genes†Effective atomic size in structural unit of ionic crystals. Science China Technological Sciences, 2019, 62, 849-855.	4.0	6
189	An Electrically Renewable Air Filter with Integrated 3D Nanowire Networks. Advanced Materials Technologies, 2019, 4, 1900101.	5.8	14
190	Discovering unusual structures from exception using big data and machine learning techniques. Science Bulletin, 2019, 64, 612-616.	9.0	28
191	Synergistic effect of charge transfer and short H-bonding on nanocatalyst surface for efficient oxygen evolution reaction. Nano Energy, 2019, 59, 443-452.	16.0	28
192	Insights into the structural evolution and Li/O loss in high-Ni layered oxide cathodes. Nano Energy, 2019, 59, 327-335.	16.0	25
193	Probing into the origin of an electronic conductivity surge in a garnet solid-state electrolyte. Journal of Materials Chemistry A, 2019, 7, 22898-22902.	10.3	50
194	Tuning mixed-phase Nb-doped titania films for high-performance photocatalysts with enhanced whole-spectrum light absorption. Catalysis Science and Technology, 2019, 9, 6027-6036.	4.1	2
195	Zr vacancy interfaces: an effective strategy for collaborative optimization of ZrNiSn-based thermoelectric performance. Journal of Materials Chemistry A, 2019, 7, 26053-26061.	10.3	16
196	In-situ and selectively laser reduced graphene oxide sheets as excellent conductive additive for high rate capability LiFePO4 lithium ion batteries. Journal of Power Sources, 2019, 412, 677-682.	7.8	27
197	In situ quantification of interphasial chemistry in Li-ion battery. Nature Nanotechnology, 2019, 14, 50-56.	31.5	373
198	A MOF-based single-ion Zn2+ solid electrolyte leading to dendrite-free rechargeable Zn batteries. Nano Energy, 2019, 56, 92-99.	16.0	227

#	Article	IF	CITATIONS
199	High Reversibility of Lattice Oxygen Redox Quantified by Direct Bulk Probes of Both Anionic and Cationic Redox Reactions. Joule, 2019, 3, 518-541.	24.0	225
200	Fingerprint Oxygen Redox Reactions in Batteries through High-Efficiency Mapping of Resonant Inelastic X-ray Scattering. Condensed Matter, 2019, 4, 5.	1.8	44
201	Revealing the Degradation Mechanism of LiMn _{<i>x</i>} Fe _{1–<i>x</i>} PO ₄ by the Single-Particle Electrochemistry Method. ACS Applied Materials & Interfaces, 2019, 11, 957-962.	8.0	24
202	Composite electrolytes of pyrrolidone-derivatives-PEO enable to enhance performance of all solid state lithium-ion batteries. Electrochimica Acta, 2019, 293, 25-29.	5.2	37
203	High-ion-energy and low-temperature deposition of diamond-like carbon (DLC) coatings with pulsed kV bias. Surface and Coatings Technology, 2019, 365, 152-157.	4.8	21
204	Tuning Superhydrophobic Materials with Negative Surface Energy Domains. Research, 2019, 2019, 1391804.	5.7	15
205	Temperature Effect on Co-Based Catalysts in Oxygen Evolution Reaction. Inorganic Chemistry, 2018, 57, 2766-2772.	4.0	54
206	High-Performance Anode Materials for Rechargeable Lithium-Ion Batteries. Electrochemical Energy Reviews, 2018, 1, 35-53.	25.5	514
207	Effective atomic interface engineering in Bi2Te2.7Se0.3 thermoelectric material by atomic-layer-deposition approach. Nano Energy, 2018, 49, 257-266.	16.0	49
208	Gate-tunable interfacial properties of in-plane ML MX ₂ 1T′–2H heterojunctions. Journal of Materials Chemistry C, 2018, 6, 5651-5661.	5.5	54
209	Insight into the origin of lithium/nickel ions exchange in layered Li(NixMnyCoz)O2 cathode materials. Nano Energy, 2018, 49, 77-85.	16.0	99
210	Engineering Fast Ion Conduction and Selective Cation Channels for a Highâ€Rate and Highâ€Voltage Hybrid Aqueous Battery. Angewandte Chemie, 2018, 130, 7164-7168.	2.0	12
211	Insight into fast ion migration kinetics of a new hybrid single Li-ion conductor based on aluminate complexes for solid-state Li-ion batteries. Nanoscale, 2018, 10, 5975-5984.	5.6	25
212	Inorganic Aromaticity of Mn ₆ -Ring Cluster in Layered Li(Ni _{0.5} Mn _{0.5})O ₂ . Journal of Physical Chemistry C, 2018, 122, 4125-4132.	3.1	10
213	Low-surface-area nitrogen doped carbon nanomaterials for advanced sodium ion batteries. Chemical Communications, 2018, 54, 2142-2145.	4.1	24
214	Biomimetic Bipolar Microcapsules Derived from <i>Staphylococcus aureus</i> for Enhanced Properties of Lithium–Sulfur Battery Cathodes. Advanced Energy Materials, 2018, 8, 1702373.	19.5	106
215	Challenges in Developing Electrodes, Electrolytes, and Diagnostics Tools to Understand and Advance Sodiumâ€ion Batteries. Advanced Energy Materials, 2018, 8, 1702403.	19.5	221
216	Mutual Independence Ensured Long-Term Cycling Stability: Template-Free Electrodeposited Sn ₄ Ni ₃ Nanoparticles as Anode Material for Lithium-Ion Batteries. ACS Applied Energy Materials, 2018, 1, 312-318.	5.1	5

#	Article	IF	CITATIONS
217	Conductive Nb-doped TiO ₂ thin films with whole visible absorption to degrade pollutants. Catalysis Science and Technology, 2018, 8, 1357-1365.	4.1	30
218	Wannier Koopmans Method Calculations of 2D Material Band Gaps. Journal of Physical Chemistry Letters, 2018, 9, 281-285.	4.6	12
219	A Conductive Binder for High-Performance Sn Electrodes in Lithium-Ion Batteries. ACS Applied Materials & Interfaces, 2018, 10, 1672-1677.	8.0	40
220	Breathing and oscillating growth of solid-electrolyte-interphase upon electrochemical cycling. Chemical Communications, 2018, 54, 814-817.	4.1	47
221	A versatile single molecular precursor for the synthesis of layered oxide cathode materials for Li-ion batteries. Chemical Communications, 2018, 54, 1331-1334.	4.1	11
222	Boosting interfacial Li+ transport with a MOF-based ionic conductor for solid-state batteries. Nano Energy, 2018, 49, 580-587.	16.0	122
223	Engineering Fast Ion Conduction and Selective Cation Channels for a Highâ€Rate and Highâ€Voltage Hybrid Aqueous Battery. Angewandte Chemie - International Edition, 2018, 57, 7046-7050.	13.8	71
224	Insight into fast Li diffusion in Li-excess spinel lithium manganese oxide. Journal of Materials Chemistry A, 2018, 6, 9893-9898.	10.3	51
225	Touching the theoretical capacity: synthesizing cubic LiTi ₂ (PO ₄) ₃ /C nanocomposites for high-performance lithium-ion battery. Nanoscale, 2018, 10, 6282-6287.	5.6	11
226	High-performance aqueous symmetric sodium-ion battery using NASICON-structured Na2VTi(PO4)3. Nano Research, 2018, 11, 490-498.	10.4	92
227	Mechanisms and properties of ion-transport in inorganic solid electrolytes. Energy Storage Materials, 2018, 10, 139-159.	18.0	267
228	Electrical contacts in monolayer blue phosphorene devices. Nano Research, 2018, 11, 1834-1849.	10.4	55
229	Self-assembled N-graphene nanohollows enabling ultrahigh energy density cathode for Li–S batteries. Nanoscale, 2018, 10, 386-395.	5.6	55
230	Asymmetric K/Li-Ion Battery Based on Intercalation Selectivity. ACS Energy Letters, 2018, 3, 65-71.	17.4	36
231	An open holey structure enhanced rate capability in a NaTi ₂ (PO ₄) ₃ /C nanocomposite and provided ultralong-life sodium-ion storage. Nanoscale, 2018, 10, 958-963.	5.6	41
232	Short Hydrogen Bonds on Reconstructed Nanocrystal Surface Enhance Oxygen Evolution Activity. ACS Catalysis, 2018, 8, 466-473.	11.2	20
233	A Metal–Organicâ€Frameworkâ€Based Electrolyte with Nanowetted Interfaces for Highâ€Energyâ€Density Solidâ€State Lithium Battery. Advanced Materials, 2018, 30, 1704436.	21.0	272
234	An ordered mesoporous silica framework based electrolyte with nanowetted interfaces for solid-state lithium batteries. Journal of Materials Chemistry A, 2018, 6, 21280-21286.	10.3	26

#	Article	IF	CITATIONS
235	Enhanced lithium dendrite suppressing capability enabled by a solid-like electrolyte with different-sized nanoparticles. Chemical Communications, 2018, 54, 13060-13063.	4.1	25
236	Activate metallic copper as high-capacity cathode for lithium-ion batteries via nanocomposite technology. Nano Energy, 2018, 54, 59-65.	16.0	22
237	n-Type Ohmic contact and p-type Schottky contact of monolayer InSe transistors. Physical Chemistry Chemical Physics, 2018, 20, 24641-24651.	2.8	33
238	Understanding Thermodynamic and Kinetic Contributions in Expanding the Stability Window of Aqueous Electrolytes. CheM, 2018, 4, 2872-2882.	11.7	187
239	Mechanism of Exact Transition between Cationic and Anionic Redox Activities in Cathode Material Li ₂ FeSiO ₄ . Journal of Physical Chemistry Letters, 2018, 9, 6262-6268.	4.6	24
240	Spectroscopic Signature of Oxidized Oxygen States in Peroxides. Journal of Physical Chemistry Letters, 2018, 9, 6378-6384.	4.6	80
241	Sub-5 nm monolayer black phosphorene tunneling transistors. Nanotechnology, 2018, 29, 485202.	2.6	21
242	Cationic Ordering Coupled to Reconstruction of Basic Building Units during Synthesis of High-Ni Layered Oxides. Journal of the American Chemical Society, 2018, 140, 12484-12492.	13.7	113
243	n- and p-type ohmic contacts at monolayer gallium nitride–metal interfaces. Physical Chemistry Chemical Physics, 2018, 20, 24239-24249.	2.8	13
244	Selfâ€Assembly of Antisite Defectless nanoâ€LiFePO ₄ @C/Reduced Graphene Oxide Microspheres for Highâ€Performance Lithiumâ€ion Batteries. ChemSusChem, 2018, 11, 2255-2261.	6.8	25
245	Interfacial Properties of Monolayer SnS–Metal Contacts. Journal of Physical Chemistry C, 2018, 122, 12322-12331.	3.1	15
246	Tuning nanosheet Fe ₂ O ₃ photoanodes with C ₃ N ₄ and p-type CoO _x decoration for efficient and stable water splitting. Catalysis Science and Technology, 2018, 8, 3144-3150.	4.1	15
247	Tuning Electronic Push/Pull of Ni-Based Hydroxides To Enhance Hydrogen and Oxygen Evolution Reactions for Water Splitting. ACS Catalysis, 2018, 8, 5621-5629.	11.2	146
248	Tuning SnSe/SnS hetero-interfaces to enhance thermoelectric performance. Functional Materials Letters, 2018, 11, 1850069.	1.2	10
249	Spontaneous valley splitting and valley pseudospin field effect transistors of monolayer VAgP ₂ Se ₆ . Nanoscale, 2018, 10, 13986-13993.	5.6	50
250	Conductive Binder for Si Anode with Boosted Charge Transfer Capability via n-Type Doping. ACS Applied Materials & Interfaces, 2018, 10, 27795-27800.	8.0	49
251	FeCoNi sulphide-derived nanodots as electrocatalysts for efficient oxygen evolution reaction. Functional Materials Letters, 2018, 11, 1850058.	1.2	4
252	Monolayer tellurene–metal contacts. Journal of Materials Chemistry C, 2018, 6, 6153-6163.	5.5	81

#	Article	IF	CITATIONS
253	Molecular dynamics study on the microstructure of CH ₃ COOLi solutions with different concentrations. Functional Materials Letters, 2018, 11, 1850075.	1.2	1
254	Tuning Cobalt and Nitrogen Coâ€Đoped Carbon to Maximize Catalytic Sites on a Superabsorbent Resin for Efficient Oxygen Reduction. ChemSusChem, 2018, 11, 3631-3639.	6.8	20
255	A heterobimetallic single-source precursor enabled layered oxide cathode for sodium-ion batteries. Chemical Communications, 2018, 54, 10714-10717.	4.1	7
256	Photocharging and Band Gap Narrowing Effects on the Performance of Plasmonic Photoelectrodes in Dye-Sensitized Solar Cells. ACS Applied Materials & Interfaces, 2018, 10, 31374-31383.	8.0	20
257	Elemental-sensitive Detection of the Chemistry in Batteries through Soft X-ray Absorption Spectroscopy and Resonant Inelastic X-ray Scattering. Journal of Visualized Experiments, 2018, , .	0.3	10
258	Ab initio identification of the Li-rich phase in LiFePO4. Physical Chemistry Chemical Physics, 2018, 20, 17497-17503.	2.8	10
259	In-situ activation for optimizing meso-/microporous structure of hollow carbon shells for supercapacitors. Functional Materials Letters, 2018, 11, 1850049.	1.2	3
260	Many-Body Effect and Device Performance Limit of Monolayer InSe. ACS Applied Materials & Interfaces, 2018, 10, 23344-23352.	8.0	98
261	Fe-Cluster Pushing Electrons to N-Doped Graphitic Layers with Fe ₃ C(Fe) Hybrid Nanostructure to Enhance O ₂ Reduction Catalysis of Zn-Air Batteries. ACS Applied Materials & Interfaces, 2017, 9, 4587-4596.	8.0	117
262	Graphene Quantum Dots Embedded in Bi ₂ Te ₃ Nanosheets To Enhance Thermoelectric Performance. ACS Applied Materials & Interfaces, 2017, 9, 3677-3685.	8.0	78
263	Hexagonal Zn _{1â^'x} Cd _x S (0.2 ≤ ≤) solid solution photocatalysts for H ₂ generation from water. Catalysis Science and Technology, 2017, 7, 982-987.	4.1	47
264	Nanofiber networks of Na ₃ V ₂ (PO ₄) ₃ as a cathode material for high performance all-solid-state sodium-ion batteries. Journal of Materials Chemistry A, 2017, 5, 5273-5277.	10.3	64
265	Hybrid n-type Sn _{1â^'x} Ta _x O ₂ nanowalls bonded with graphene-like layers as high performance electrocatalysts for flexible energy conversion devices. Journal of Materials Chemistry A, 2017, 5, 6884-6892.	10.3	8
266	Fast Diffusion of O ₂ on Nitrogen-Doped Graphene to Enhance Oxygen Reduction and Its Application for High-Rate Zn–Air Batteries. ACS Applied Materials & Interfaces, 2017, 9, 7125-7130.	8.0	52
267	Optimized mesopores enabling enhanced rate performance in novel ultrahigh surface area meso-/microporous carbon for supercapacitors. Nano Energy, 2017, 33, 453-461.	16.0	210
268	Depolarization effect to enhance the performance of lithium ions batteries. Nano Energy, 2017, 33, 497-507.	16.0	79
269	High-efficiency <i>in situ</i> resonant inelastic x-ray scattering (iRIXS) endstation at the Advanced Light Source. Review of Scientific Instruments, 2017, 88, 033106.	1.3	107
270	Novel conductive binder for high-performance silicon anodes in lithium ion batteries. Nano Energy, 2017, 36, 206-212.	16.0	178

#	Article	IF	CITATIONS
271	In-situ mass-electrochemical study of surface redox potential and interfacial chemical reactions of Li(Na)FePO 4 nanocrystals for Li(Na)-ion batteries. Nano Energy, 2017, 37, 90-97.	16.0	20
272	A novel MoS ₂ -based hybrid film as the back electrode for high-performance thin film solar cells. RSC Advances, 2017, 7, 23415-23421.	3.6	8
273	Multifunctional Co 3 S 4 @sulfur nanotubes for enhanced lithium-sulfur battery performance. Nano Energy, 2017, 37, 7-14.	16.0	335
274	Co ₃ O _{4â^îî′} Quantum Dots As a Highly Efficient Oxygen Evolution Reaction Catalyst for Water Splitting. ACS Applied Materials & Interfaces, 2017, 9, 16159-16167.	8.0	104
275	Controllable synthesis of LiFePO ₄ in different polymorphs and study of the reaction mechanism. Journal of Materials Chemistry A, 2017, 5, 14294-14300.	10.3	25
276	Monolayer Bismuthene-Metal Contacts: A Theoretical Study. ACS Applied Materials & Interfaces, 2017, 9, 23128-23140.	8.0	73
277	Novel Ag-doped glass frits for high-efficiency crystalline silicon solar cells. Chemical Communications, 2017, 53, 6239-6242.	4.1	12
278	Effect of excess lithium in LiMn2O4 and Li1.15Mn1.85O4 electrodes revealed by quantitative analysis of soft X-ray absorption spectroscopy. Applied Physics Letters, 2017, 110, .	3.3	21
279	Excellent corrosion resistance of P and Fe modified micro-arc oxidation coating on Al alloy. Journal of Alloys and Compounds, 2017, 710, 452-459.	5.5	53
280	Novel hybrid Si nanocrystals embedded in a conductive SiO _x @C matrix from one single precursor as a high performance anode material for lithium-ion batteries. Journal of Materials Chemistry A, 2017, 5, 7026-7034.	10.3	55
281	Optimizing CdTe–metal interfaces for high performance solar cells. Journal of Materials Chemistry A, 2017, 5, 7118-7124.	10.3	18
282	The synergistic effect achieved by combining different nitrogen-doped carbon shells for high performance capacitance. Chemical Communications, 2017, 53, 857-860.	4.1	16
283	Olivine FePO ₄ Cathode Material for Rechargeable Mg-Ion Batteries. Inorganic Chemistry, 2017, 56, 13411-13416.	4.0	27
284	Role of Superexchange Interaction on Tuning of Ni/Li Disordering in Layered Li(Ni _{<i>x</i>} Mn _{<i>y</i>} Co _{<i>z</i>})O ₂ . Journal of Physical Chemistry Letters, 2017, 8, 5537-5542.	4.6	125
285	In situ probing of interfacial kinetics for studying the electrochemical properties of active nano/micro-particles and the state of Li-ion batteries. Journal of Materials Chemistry A, 2017, 5, 22598-22606.	10.3	7
286	First-Principles Study of Cu ₉ S ₅ : A Novel p-Type Conductive Semiconductor. Journal of Physical Chemistry C, 2017, 121, 23317-23323.	3.1	31
287	In Situ Wrapping Si Nanoparticles with 2D Carbon Nanosheets as High-Areal-Capacity Anode for Lithium-Ion Batteries. ACS Applied Materials & Interfaces, 2017, 9, 38159-38164.	8.0	83
288	Synthetic Control of Kinetic Reaction Pathway and Cationic Ordering in Highâ€Ni Layered Oxide Cathodes. Advanced Materials, 2017, 29, 1606715.	21.0	127

#	Article	IF	CITATIONS
289	Pressure-induced abnormal insulating state in triangular layered cobaltite Li _x CoO ₂ (x = 0.9). Journal of Materials Chemistry A, 2017, 5, 19390-19397.	10.3	9
290	Flexible Composite Solid Electrolyte Facilitating Highly Stable "Soft Contacting―Li–Electrolyte Interface for Solid State Lithiumâ€Ion Batteries. Advanced Energy Materials, 2017, 7, 1701437.	19.5	237
291	Nanocrystals generated under tensile stress in metallic glasses with phase selectivity. Nanoscale, 2017, 9, 15542-15549.	5.6	3
292	Ultrahigh surface area meso/microporous carbon formed with self-template for high-voltage aqueous supercapacitors. Journal of Power Sources, 2017, 365, 362-371.	7.8	28
293	Effect of sulfur-containing additives on the formation of a solid-electrolyte interphase evaluated by in situ AFM and ex situ characterizations. Journal of Materials Chemistry A, 2017, 5, 19364-19370.	10.3	33
294	Excess Li-Ion Storage on Reconstructed Surfaces of Nanocrystals To Boost Battery Performance. Nano Letters, 2017, 17, 6018-6026.	9.1	53
295	Electrical Contacts in Monolayer Arsenene Devices. ACS Applied Materials & Interfaces, 2017, 9, 29273-29284.	8.0	76
296	Controllable Formation of (004)-Orientated Nb:TiO ₂ for High-Performance Transparent Conductive Oxide Thin Films with Tunable Near-Infrared Transmittance. ACS Applied Materials & Interfaces, 2017, 9, 29021-29029.	8.0	20
297	Wannier Koopman method calculations of the band gaps of alkali halides. Applied Physics Letters, 2017, 111, .	3.3	10
298	How Solid-Electrolyte Interphase Forms in Aqueous Electrolytes. Journal of the American Chemical Society, 2017, 139, 18670-18680.	13.7	365
299	Tuning Li-Ion Diffusion in α-LiMn _{1–<i>x</i>} Fe _{<i>x</i>} PO ₄ Nanocrystals by Antisite Defects and Embedded β-Phase for Advanced Li-Ion Batteries. Nano Letters, 2017, 17, 4934-4940.	9.1	38
300	In-situ self-polymerization restriction to form core-shell LiFePO4/C nanocomposite with ultrafast rate capability for high-power Li-ion batteries. Nano Energy, 2017, 39, 346-354.	16.0	58
301	Optimized hetero-interfaces by tuning 2D SnS2 thickness in Bi2Te2.7Se0.3/SnS2 nanocomposites to enhance thermoelectric performance. Nano Energy, 2017, 39, 297-305.	16.0	74
302	In Situ Probing and Synthetic Control of Cationic Ordering in Niâ€Rich Layered Oxide Cathodes. Advanced Energy Materials, 2017, 7, 1601266.	19.5	200
303	Singleâ€Particle Performances and Properties of LiFePO ₄ Nanocrystals for Liâ€lon Batteries. Advanced Energy Materials, 2017, 7, 1601894.	19.5	41
304	3Dâ€Printed Cathodes of LiMn _{1â^'} <i>_x</i> Fe <i>_x</i> PO ₄ Nanocrystals Achieve Both Ultrahigh Rate and High Capacity for Advanced Lithiumâ€Ion Battery. Advanced Energy Materials, 2016, 6, 1600856.	19.5	157
305	Optimized Temperature Effect of Liâ€ŀon Diffusion with Layer Distance in Li(Ni <i>_x</i> Mn <i>_y</i> Co <i>_z</i>)O ₂ Cathode Materials for High Performance Liâ€ŀon Battery. Advanced Energy Materials, 2016, 6, 1501309.	19.5	182
306	A novel p-type and metallic dual-functional Cu–Al ₂ O ₃ ultra-thin layer as the back electrode enabling high performance of thin film solar cells. Chemical Communications, 2016, 52, 10708-10711.	4.1	10

#	Article	IF	CITATIONS
307	Ni and Co Segregations on Selective Surface Facets and Rational Design of Layered Lithium Transitionâ€Metal Oxide Cathodes. Advanced Energy Materials, 2016, 6, 1502455.	19.5	100
308	The role of nanotechnology in the development of battery materials for electric vehicles. Nature Nanotechnology, 2016, 11, 1031-1038.	31.5	581
309	Transition metal redox and Mn disproportional reaction in LiMn0.5Fe0.5PO4 electrodes cycled with aqueous electrolyte. Applied Physics Letters, 2016, 109, .	3.3	13
310	A Novel Real-Time State-of-Health and State-of-Charge Co-Estimation Method for LiFePO 4 Battery. Chinese Physics Letters, 2016, 33, 078201.	3.3	6
311	3D-printing Ag-line of front-electrodes with optimized size and interface to enhance performance of Si solar cells. RSC Advances, 2016, 6, 51871-51876.	3.6	18
312	The formation and mechanism of nano-monocrystalline γ-Fe ₂ O ₃ with graphene-shell for high-performance lithium ion batteries. RSC Advances, 2016, 6, 51777-51782.	3.6	12
313	Revealing the nanodomain structure of silicon oxycarbide via preferential etching and pore analysis. Functional Materials Letters, 2016, 09, 1650043.	1.2	6
314	Core–Shell Sn–Ni–Cu-Alloy@Carbon Nanorods to Array as Three-Dimensional Anode by Nanoelectrodeposition for High-Performance Lithium Ion Batteries. ACS Applied Materials & Interfaces, 2016, 8, 12221-12227.	8.0	51
315	Depolarization effects of Li ₂ FeSiO ₄ nanocrystals wrapped in different conductive carbon networks as cathodes for high performance lithium-ion batteries. RSC Advances, 2016, 6, 47723-47729.	3.6	19
316	Few-Layer Tin Sulfide: A New Black-Phosphorus-Analogue 2D Material with a Sizeable Band Gap, Odd–Even Quantum Confinement Effect, and High Carrier Mobility. Journal of Physical Chemistry C, 2016, 120, 22663-22669.	3.1	130
317	Aligned Li ⁺ Tunnels in Core–Shell Li(Ni _{<i>x</i>} Mn _{<i>y</i>} Co _{<i>z</i>})O ₂ @LiFePO _{4Enhances Its High Voltage Cycling Stability as Li-ion Battery Cathode. Nano Letters, 2016, 16, 6357-6363.}	o>9 . 1	117
318	Interfacial properties of stanene–metal contacts. 2D Materials, 2016, 3, 035020.	4.4	26
319	2D hetero-nanosheets to enable ultralow thermal conductivity by all scale phonon scattering for highly thermoelectric performance. Nano Energy, 2016, 30, 780-789.	16.0	54
320	Cascading Boost Effect on the Capacity of Nitrogen-Doped Graphene Sheets for Li- and Na-Ion Batteries. ACS Applied Materials & Interfaces, 2016, 8, 26722-26729.	8.0	46
321	Tuning of Thermal Stability in Layered Li(Ni _{<i>x</i>} Mn _{<i>y</i>} Co _{<i>z</i>})O ₂ . Journal of the American Chemical Society, 2016, 138, 13326-13334.	13.7	178
322	Soft-contact conductive carbon enabling depolarization of LiFePO4 cathodes to enhance both capacity and rate performances of lithium ion batteries. Journal of Power Sources, 2016, 331, 232-239.	7.8	41
323	Quantitative probe of the transition metal redox in battery electrodes through soft x-ray absorption spectroscopy. Journal Physics D: Applied Physics, 2016, 49, 413003.	2.8	90
324	Novel Organic–Inorganic Hybrid Electrolyte to Enable LiFePO ₄ Quasi-Solid-State Li-Ion Batteries Performed Highly around Room Temperature. ACS Applied Materials & Interfaces, 2016, 8, 31273-31280.	8.0	67

#	Article	IF	CITATIONS
325	Few-Layer Fe ₃ (PO ₄) ₂ ·8H ₂ O: Novel H-Bonded 2D Material and Its Abnormal Electronic Properties. Journal of Physical Chemistry C, 2016, 120, 26278-26283.	3.1	2
326	Interfacial Properties of Monolayer MoSe ₂ –Metal Contacts. Journal of Physical Chemistry C, 2016, 120, 13063-13070.	3.1	70
327	Pre-Lithiation of Li(Ni _{1-<i>x</i>} O ₂ Materials Enabling Enhancement of Performance for Li-Ion Battery. ACS Applied Materials & amp; Interfaces. 2016. 8. 15361-15368.	8.0	32
328	Tuning Cu dopant of Zn0.5Cd0.5S nanocrystals enables high-performance photocatalytic H2 evolution from water splitting under visible-light irradiation. Nano Energy, 2016, 26, 405-416.	16.0	78
329	Novel p-Type Conductive Semiconductor Nanocrystalline Film as the Back Electrode for High-Performance Thin Film Solar Cells. Nano Letters, 2016, 16, 1218-1223.	9.1	30
330	Core–shell nano-FeS ₂ @N-doped graphene as an advanced cathode material for rechargeable Li-ion batteries. Chemical Communications, 2016, 52, 986-989.	4.1	84
331	High-performance NaFePO ₄ formed by aqueous ion-exchange and its mechanism for advanced sodium ion batteries. Journal of Materials Chemistry A, 2016, 4, 4882-4892.	10.3	129
332	Mesoporous and carbon hybrid structures from layered molecular precursors for Li-ion battery application: the case of β-In2S3. Chemical Communications, 2016, 52, 4788-4791.	4.1	8
333	Tuning structural stability and lithium-storage properties by d -orbital hybridization substitution in full tetrahedron Li 2 FeSiO 4 nanocrystal. Nano Energy, 2016, 20, 117-125.	16.0	44
334	Storage and Effective Migration of Li-Ion for Defected β-LiFePO ₄ Phase Nanocrystals. Nano Letters, 2016, 16, 601-608.	9.1	31
335	Rectification and tunneling effects enabled by Al2O3 atomic layer deposited on back contact of CdTe solar cells. Applied Physics Letters, 2015, 107, .	3.3	27
336	FeOxand Si nano-dots as dual Li-storage centers bonded with graphene for high performance lithium ion batteries. Nanoscale, 2015, 7, 14344-14350.	5.6	8
337	Fast rechargeable all-solid-state lithium ion batteries with high capacity based on nano-sized Li2FeSiO4 cathode by tuning temperature. Nano Energy, 2015, 16, 112-121.	16.0	37
338	Kinetics Tuning of Li-Ion Diffusion in Layered Li(Ni _{<i>x</i>} Mn _{<i>y</i>} Co _{<i>z</i>})O ₂ . Journal of the American Chemical Society, 2015, 137, 8364-8367.	13.7	292
339	Atomic-Resolution Visualization of Distinctive Chemical Mixing Behavior of Ni, Co, and Mn with Li in Layered Lithium Transition-Metal Oxide Cathode Materials. Chemistry of Materials, 2015, 27, 5393-5401.	6.7	108
340	Prelithiation Activates Li(Ni _{0.5} Mn _{0.3} Co _{0.2})O ₂ for High Capacity and Excellent Cycling Stability. Nano Letters, 2015, 15, 5590-5596.	9.1	68
341	Gradual-order enhanced stability: a frozen section of electrospun nanofibers for energy storage. Nanoscale, 2015, 7, 8715-8719.	5.6	19
342	Silicene nanomesh. Scientific Reports, 2015, 5, 9075.	3.3	42

#	Article	IF	CITATIONS
343	2D hybrid anode based on SnS nanosheet bonded with graphene to enhance electrochemical performance for lithium-ion batteries. RSC Advances, 2015, 5, 46941-46946.	3.6	76
344	Li ₂ FeSiO ₄ nanorods bonded with graphene for high performance batteries. Journal of Materials Chemistry A, 2015, 3, 9601-9608.	10.3	59
345	A core–shell nanohollow-γ-Fe ₂ O ₃ @graphene hybrid prepared through the Kirkendall process as a high performance anode material for lithium ion batteries. Chemical Communications, 2015, 51, 7855-7858.	4.1	76
346	Enhancing the High-Voltage Cycling Performance of LiNi _{0.5} Mn _{0.3} Co _{0.2} O ₂ by Retarding Its Interfacial Reaction with an Electrolyte by Atomic-Layer-Deposited Al ₂ O ₃ . ACS Applied Materials & amp; Interfaces, 2015, 7, 25105-25112.	8.0	158
347	Janus Solid–Liquid Interface Enabling Ultrahigh Charging and Discharging Rate for Advanced Lithium-Ion Batteries. Nano Letters, 2015, 15, 6102-6109.	9.1	90
348	Sn(ii,iv) steric and electronic structure effects enable self-selective doping on Fe/Si-sites of Li2FeSiO4 nanocrystals for high performance lithium ion batteries. Journal of Materials Chemistry A, 2015, 3, 24437-24445.	10.3	15
349	γ-Fe ₂ O ₃ Nanocrystalline Microspheres with Hybrid Behavior of Battery-Supercapacitor for Superior Lithium Storage. ACS Applied Materials & Interfaces, 2015, 7, 26284-26290.	8.0	58
350	Formation of mono/bi-layer iron phosphate and nucleation of LiFePO 4 nano-crystals from amorphous 2D sheets in charge/discharge process for cathode in high-performance Li-ion batteries. Nano Energy, 2015, 18, 187-195.	16.0	30
351	Depolarized and Fully Active Cathode Based on Li(Ni _{0.5} Co _{0.2} Mn _{0.3})O ₂ Embedded in Carbon Nanotube Network for Advanced Batteries. Nano Letters, 2014, 14, 4700-4706.	9.1	95
352	Ultralow-limit gas detection in nano-dumbbell polymer sensor via electrospinning. Nanoscale, 2013, 5, 1803.	5.6	41
353	Nonlinear optical organic co-crystals of merocyanine dyes and phenolic derivatives with short hydrogen bonds. Chemical Physics, 1999, 245, 377-394.	1.9	31
354	Novel electro-optic molecular cocrystals with ideal chromophoric orientation and large second-order optical nonlinearities. Journal of the Optical Society of America B: Optical Physics, 1998, 15, 426.	2.1	51
355	A highly efficient organic second-order nonlinear optical crystal based on a donor-acceptor substituted 4-nitrophenylhydrazone. Applied Physics Letters, 1997, 71, 2064-2066.	3.3	16
356	Self-assembly of an acentric co-crystal of a highly hyperpolarizable merocyanine dye with optimized alignment for nonlinear optics. Advanced Materials, 1997, 9, 554-557.	21.0	44
357	Novel Organic Crystals for Nonlinear and Electro-Optics. , 1997, , 279-296.		5
358	A Novel and Perfectly Aligned Highly Electroâ^'Optic Organic Cocrystal of a Merocyanine Dye and 2,4-Dihydroxybenzaldehyde. Journal of the American Chemical Society, 1996, 118, 6315-6316.	13.7	99
359	Five-membered heteroaromatic hydrazone derivatives for second-order nonlinear optics. Advanced Materials, 1996, 8, 416-420.	21.0	49
360	Non-classical donor-acceptor chromophores for second order nonlinear optics. Advanced Materials, 1996, 8, 677-680.	21.0	127

#	Article	IF	CITATIONS
361	Balancing Stability and Li-ion Conductivity of Li10SiP2O12 for Solid-State Electrolytes with Assistance of body-centered cubic oxygen framework. Journal of Materials Chemistry A, 0, , .	10.3	2